ACS APPLIED MATERIALS & INTERFACES

Research Article

www.acsami.org

Fabrication and Short-Term in Vivo Performance of a Natural Elastic Lamina–Polymeric Hybrid Vascular Graft

Connor W. McCarthy,[†] Danielle C. Ahrens,[†] David Joda,[†] Tyler E. Curtis,[†] Patrick K. Bowen,[‡] Roger J. Guillory II,[†] Shu Q. Liu,[§] Feng Zhao,[†] Megan C. Frost,[†] and Jeremy Goldman*[,†]

[†]Department of Biomedical Engineering and [‡]Department of Materials Science and Engineering, Michigan Technological University, Houghton, Michigan 49931, United States

[§]Biomedical Engineering Department, Northwestern University, Evanston, Illinois 60208, United States

Supporting Information

ABSTRACT: Although significant advances have been made in the development of artificial vascular grafts, small-diameter grafts still suffer from excessive platelet activation, thrombus formation, smooth muscle cell intimal hyperplasia, and high occurrences of restenosis. Recent discoveries demonstrating the excellent blood-contacting properties of the natural elastic lamina have raised the possibility that an acellular elastic lamina could effectively serve as a patent blood-contacting surface in engineered vascular grafts. However, the elastic lamina alone lacks the requisite mechanical properties to function as a viable vascular graft. Here, we have screened a wide range of biodegradable and biostable medical-grade polymers for their ability to adhere to the outer surface of the elastic lamina and allow cellular repopulation following engraftment in the rat abdominal aorta. We demonstrate a novel method for the fabrication of elastic lamina–polymeric hybrid small-diameter vascular grafts and identify poly(ether urethane) (PEU 1074A) as ideal for this purpose. In vivo results demonstrate graft patency over 21 days, with low thrombus formation, mild inflammation, and the general absence of smooth muscle cell hyperplasia on the graft's luminal surface. The results provide a new direction for developing small-diameter vascular grafts that are mass-producible, shelf-stable, and universally compatible due to a lack of immune response and inhibit the in-graft restenosis response that is common to nonautologous materials.

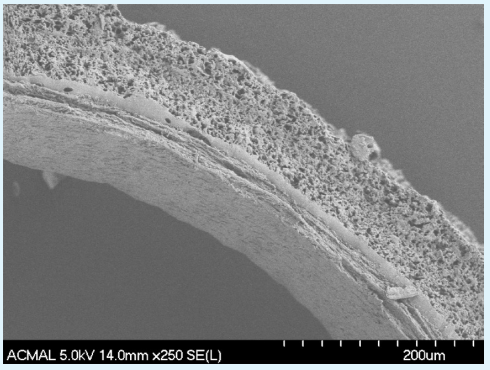

KEYWORDS: *elastic lamina, blood-contacting, small-diameter vascular graft, polymeric scaffold, neointimal hyperplasia, restenosis*

1. INTRODUCTION

Small-diameter blood vessels are required during coronary artery bypass grafting (CABG) to circumvent occluded coronary arteries. Currently, autologous arteries and veins used as grafts for the approximately 500 000 CABG procedures performed in the United States each year[1,2] represent the gold standard. However, a significant number of patients (~33%) are not able to make use of autologous vessels due to preexisting conditions.[3] Presently, there is no engineered vascular graft that is reliably able to replace autologous blood vessels in application.

Both synthetic and natural vascular graft materials have been in use for several decades in large-diameter arteries.[2−4] Synthetic examples include polymeric grafts fabricated from poly(tetrafluoroethylene) (PTFE/ePTFE), poly(ethylene terephthalate) (Dacron), and polyurethanes.[4,5] However, small-diameter synthetic vascular grafts are susceptible to high rates of failure due to thrombosis, intimal hyperplasia, and restenosis.[6−12] Natural, tissue-engineered blood vessels (TEBVs) are under development and have achieved some clinical success.[1,13] However, their expense, long fabrication time, short shelf life, and arduous regulatory pathway are expected to hinder their widespread clinical acceptance. Thus, there is a pressing need for small-diameter vascular substitutes that can be mass-produced, are shelf-stable over long time periods, and do not provoke excessive thrombosis or neointimal hyperplasia.

Decellularized elastic lamina, purified from the media layer of donor blood vessels, has recently been shown to possess anti-inflammatory and antithrombogenic properties. When exposed to arterial blood flow, the elastic lamina elicits lower platelet and monocyte activation, thrombosis, and smooth muscle cell proliferation than collagen-containing blood-contacting surfaces.[14−17] This has raised the prospect that the elastic lamina may substitute for a confluent endothelium in engineered acellular vascular grafts. However, despite highly promising early results with elastic lamina scaffolds, there has been a lack of progress incorporating this material into vascular grafts. This may be attributed to the high cost and low yields of synthetic elastin and recombinant tropoelastin.[18−20] Another significant

Received: December 15, 2014
Accepted: July 13, 2015
Published: July 23, 2015

DOI: 10.1021/acsami.5b03892
ACS Appl. Mater. Interfaces 2015, 7, 16202−16212

Table 1. Summary of Properties for Selected Polymers[a]

	structure	ultimate tensile strength (MPa)	ultimate elongation (%)	wetting angle (deg)
poly(glycolic acid) (PGA)	aliphatic	60−99.7[33]	1.5−20[33]	70.3[34]
poly(L-lactic acid) (PLLA)	aliphatic	50(2.4)−55(0.5)[30,31]	2.1(0.1)−8.0(0.2)[30,31]	82(2.3)[32]
polycaprolactone (PCL)	aliphatic	25.1[35]	>450[35]	69[37]
poly(carbonate urethane) 3585A	aliphatic	57.23	425	82.1[43]
poly(carbonate urethane) 4085A	aliphatic	62.05	400	82.1[43]
poly(ether urethane) SG80A	aliphatic	39.99[39]	660[39]	NDA
poly(ether urethane) 1074A	aromatic	41.37	550	82[36]
poly(ether urethane) 1085A	aromatic	48.26	450	NDA

[a]Standard deviations are given in parentheses when the data were available. NDA signifies that no data were available. Where there are no references listed, the values were obtained from the manufacturer's data sheet.

hurdle is elastin's relative insolubility, precluding the polymerization of native elastin by common solvent deposition or electrospinning methods.[21] Recent studies on the inclusion of elastin in polymeric vascular grafts have focused on soluble human recombinant tropoelastin electrospun directly into the polymer fiber scaffold[20,22] or soluble elastin derived from bovine ligamentum nuche,[23] also electrospun directly into the scaffold. In the present study, we have purified native elastic lamina scaffolds from rat donor arteries, thereby circumventing these serious challenges while maintaining the native architecture and biological properties of the elastin matrix.

Unfortunately, the decellularized elastic lamina purified from donor arteries is easily torn, lacks mechanical strength, and retains regularly segmented holes due to side-branching. In this study, we have undertaken a materials selection process to identify polymeric materials that can adhere to the elastic lamina and provide mechanical integrity and structural support. We began our development work by employing poly(glycolic acid) (PGA) and poly(L-lactic acid) (PLLA) polymers, which are widely used and well characterized,[24−28] as a proof-of-concept. Both PGA and PLLA are biodegradable aliphatic polyesters. PGA has a degradation time of approximately 2−4 weeks, while PLLA will degrade over a period of several months to several years. Both PGA (45−55%) and PLLA (37%) are considered semicrystalline materials.[25,28,29] Subsequently, polycaprolactone (PCL), poly(ether urethane)s (PEUs), and poly(carbonate urethane)s (PCUs) were selected for evaluation due to their well-accepted biocompatibility, hydrophobicity similar to that of the elastic lamina, and mechanical properties similar to those of the arterial tissue of the host[37−42] (Table 1). We then evaluated the best performing hybrid vascular graft out to 21 days, in vivo.

2. MATERIALS AND METHODS

2.1. Aorta Specimen Collection. All animal work was approved by Michigan Technological University's Internal Animal Care and Use Committee (IACUC). Rat thoracic aortas used as donor tissue were collected from Sprague−Dawley rats (Harlan Laboratories; Indianapolis, IN) euthanized with 5% inhaled isoflurane. The diaphragms were punctured, and the hearts were removed to ensure death. Thoracic aorta segments ~30 mm in length were isolated, excised, and stored in phosphate-buffered saline (PBS) (pH 7.4) at 4 °C for later use.

2.2. Polymers and Solvents. PGA was purchased from Polysciences, Inc. (Warrington, PA). PLLA was purchased from NatureWorks LLC (Blair, NE). All polyurethanes used were from the Lubrizol LifeSciences (Wickliffe, OH) polymer family and are biostable[43,44] thermoplastic polyurethanes. These included poly(ether urethane)s Tecothanes 1074A and 1085A as well as Tecoflex SG80A. The poly(carbonate urethane) compounds used in this project were also from the Lubrizol LifeSciences polymer family and included Carbothanes 3585A and 4085A. PBS, hexafluoro-2-propanol (HFIP), chloroform, dichloromethane, *N*,*N*-dimethylacetamide, acetone, Dulbecco's modified Eagle's medium (DMEM), fetal bovine serum (FBS), penicillin/streptomycin (P/S), and sodium hydroxide (NaOH) were all purchased from Sigma-Aldrich (St. Louis, MO).

2.3. Materials Development. *2.3.1. Decellularization and UV Treatment of Elastic Lamina.* Aortic specimens were processed to remove all nonelastin matrixes, leaving a purified and decellularized elastic lamina. Briefly, the aortic specimens were placed in a 50 mL conical tube immersed in PBS (pH 7.4). NaOH was added to the solution to make a basic PBS solution (pH 12.7).[14,15] They were then placed into an ultrasonic bath for 4 h at 37 °C, changing the solution every hour. The aortic specimens were rinsed in PBS (pH 7.4) to remove residual NaOH. They were then washed in DMEM with 10% (v/v) FBS and 1% (v/v) P/S for 48 h at 4 °C to remove cellular fragments and residual DNA material.

The elastic lamina matrix was modified by irradiating the outer matrix layer with ultraviolet (UV) light. UV treatment to cross-link natural matrixes has been described previously.[45] Contrary to chemical methods of cross-linking, irradiation-based treatment does not incorporate cytotoxic compounds into the matrix.[46] Some groups have reported limited degradation of matrix components after UV treatment.[47,48] Processed segments were mounted on 304 stainless steel mandrels (outer diameter of 1.65 mm) and UV irradiated with 380 ± 20 nm radiation at 1.5 W/cm^2 (Phoseon Technology; Hillsboro, OR) for 2 h. The UV source was placed 6 cm above the specimens. The specimens were rotated 90° every 30 min to ensure even exposure. A PBS (pH 7.4) bath was used to keep the specimens hydrated. The elastic lamina scaffolds were allowed to dry for 48 h after UV treatment.

2.3.2. Polymer Coating. The UV-treated elastic lamina scaffolds were coated in 1% (w/w) solutions of the selected solvent/polymer combination, listed in Table S1 (Supporting Information). An airbrush (Iwata Eclipse, Portland, OR) was used to spray-coat the scaffold with the chosen polymer solution. The airbrush was fed at 15 psi from a dry, compressed air source. The scaffold was coated with 500 μL of polymer solution at a distance of 10 cm from the brush tip. The vessels were allowed to dry overnight prior to electrospinning. Polymer adhesion to the elastic lamina was evaluated by spray-coating a sample of the UV-treated elastic lamina with each polymer and soaking the samples in PBS (pH 7.4) for 5 days at room temperature. The PBS-immersed specimens were qualitatively examined under a stereomicroscope to identify the presence of delamination.

To provide structural support, electrospun fibers were deposited over the polymer-coated elastic lamina scaffolds. Electrospinning needles were purchased from Beckton, Dickinson & Co. (Franklin Lakes, NJ). For the constructs coated in PLLA, an 8% (w/w) solution of PLLA was prepared in equal masses of chloroform and dichloromethane. For the samples coated in the polyurethane-based materials, a 5% (w/w) solution of PEU 1074A dissolved in HFIP was used. Electrospinning of the PLLA fibers was performed between 33% and 37% relative humidity, with a solution feed of 2 mL/h through a 22 gauge needle at a distance of 4.5 cm from the needle tip. The accelerating voltage used was 17 kV, and the 1.65 mm diameter mandrel rotated at 2500 rpm during collection. The poly(ether

DOI: 10.1021/acsami.5b03892
ACS Appl. Mater. Interfaces 2015, 7, 16202−16212

urethane) samples had similar parameters; however, the flow rate was decreased to 0.5 mL/h due to the change in solvent to HFIP. The samples were electrospun for 10 min to create the specific layer thickness and fiber density. The samples were treated with ethylene oxide for 12 h in an Anprolene AN74i sterilizer (Haw River, NC) prior to implantation. All samples were hydrated in sterile saline for ~5 min prior to surgery to prevent fractures during manipulation.

2.4. Electron Microscopy. Field emission scanning electron microscopy (FESEM) was used to examine the processed elastic lamina scaffolds and engineered vascular grafts using a Hitachi S-4700 field emission electron microscope (5 kV accelerating voltage, 10 μA beam current; Tokyo, Japan). Specimens were prepared for imaging by allowing them to air-dry. Final dehydration was accomplished while under vacuum in the sputter coater. Specimens were sputter coated with 5 nm of Pt/Pd on a Hummer 6.2 sputter coater (Anatech, Ltd., Denver, NC), and were stored in a desiccator prior to imaging.

2.5. Electrospun Fiber Characterization. Electrospun fibers (n = 3) were characterized manually using NIH ImageJ software after imaging on the electron microscope. Fiber diameters were determined by manually measuring individual fibers under high magnification. Fiber densities were determined by drawing a horizontal line in the image and counting the number of fibers present over the total length of the line.

2.6. Burst Pressure Testing. Vascular graft samples (n = 4) were mechanically tested to failure through burst pressure measurement. To perform the burst pressure testing, samples were fixed to hollow 304 stainless steel mandrels (1.65 mm outside diameter) with Dow Corning Silastic tubing (0.3 mm i.d., 0.64 mm o.d.; Midland, MI). The far end of the distal mandrel was capped following the removal of air from the apparatus. The hydrostatic pressure was recorded on a Fisher Scientific vacuum gauge (Pittsburgh, PA), while videos of the vessels during the test were recorded on a Nikon D3200 DSLR camera (Melville, NY). PBS (pH 7.4) was pumped into the vessel at a fixed rate of 300 μL/min by a syringe pump (Kent Scientific Genie Plus, Torrington, CT).

2.7. Mechanical Analysis. The electrospun polymer layers of the vascular grafts were mechanically tested in monotonic tension in the longitudinal direction on a Bose Electroforce 3200 series III (Eden Prairie, MN) frame with a 2 kg (19.6 N) load cell. Tubular samples were cut open longitudinally to produce sheets, which were fixed in Bose low force grips. The Bose Electroforce 3200 used in this work had a 6 mm travel limit during tensile testing. Thus, PLLA electrospun samples were tested to failure, while the highly elastic PEU 1074A electrospun fibers were tested up to the limit of the testing frame. Values affected by these limitations are denoted within the paper. Mechanical data are presented as an average of six samples ± standard deviations. Data were analyzed in Matlab R2014a (Mathworks, Natick, MA).

2.8. Surgical Procedure. Sprague–Dawley rats (Harlan Laboratories, Indianapolis, IN) anesthetized with 2.1% inhaled isoflurane in oxygen gas were implanted with ~6–8 mm long engineered vessels, as interpositional vascular grafts, using an end-to-end anastamotic technique described previously.[38] Briefly, the abdominal aorta was carefully isolated, and the proximal and distal ends were clamped to prevent blood flow. Side branches were identified and tied off to prevent blood flow within the clamped aortic segment, prior to the artery being severed midway between the two clamps. For the PLLA scaffolds that were evaluated at 1 h and 3 days (n = 1), both distal and proximal ends of the exposed, severed artery were treated with heparin in PBS (pH 7.4; 0.5 unit in ~2 μL saline) to reduce blood coagulation at the exposed collagen-containing arterial wall. However, no heparin or any other anticoagulant was used when the polyurethane-based scaffold was implanted for either 3 (n = 1) or 21 (n = 5) days. The vessel constructs were engrafted with 15–20 interrupted suture stitches (10-0 nylon suture) at each end. Blood flow was reestablished, and the grafts were evaluated for leakage. Upon re-establishment of blood flow, pulsation was observed in the host artery, both proximally and distally to the implant. The abdomen was either kept open, in the case of the 1 h PLLA specimen, or closed using a combination of sutures (for muscle) and staples (for skin), and the rat was allowed to recover for 3 or 21 days. The rats were observed for several minutes following recovery to confirm normal mobility in the hind quarters, which further indicated graft patency.

Animals were sacrificed at the designated end points by increasing the inhaled isoflurane concentration from 2.1% to 5% after the animals were fully anesthetized. The implant site was carefully isolated, and the vessels were evaluated for vascular tone and blood flow. Again, pulsation was observed in the host artery surrounding the graft. Then, under deep anesthesia, the diaphragms were punctured, the chest cavity was opened, and the heart was removed to ensure death. The grafts were collected with host artery connected at both the distal and proximal ends. A longitudinal cut was made in the collected graft to expose the internal lumen for imaging the graft surface for the single 1 h and two 3 day grafts. The five 21 day grafts were left intact and gently syringe perfused with freezing medium to both confirm patency and facilitate cryosectioning. The samples were surrounded with Polyfreeze freezing medium (Sigma-Aldrich, St. Louis, MO), snap frozen in liquid nitrogen, and stored at −80 °C until cryosectioning. A 21 day implant duration reflects the standard practice for early phase vascular graft development.[22]

2.9. Histological Preparation and Imaging. Processed elastic lamina scaffolds were imaged on an Olympus BX-51 microscope (Waltham, MA) to confirm decellularization and decollagenization prior to UV treatment, using both a fluorescent 4′,6-diamidino-2-phenylindole (DAPI) nuclear stain and a Verhoeff–Van Gieson (VVG) stain. Explanted samples were additionally stained with hematoxylin and eosin (H&E). All components for staining were purchased from Sigma-Aldrich (St. Louis, MO), with the exception of Gill's no. 3, which was purchased from Leica Biosystems (Buffalo Grove, IL). Specimens were sectioned on a Microm HM550 cryostat (Microm International GmbH, Walldorf, Germany) at a thickness of 10 μm and fixed in ethanol for 60 s.

The samples were rinsed in PBS (pH 7.4) three times prior to undergoing staining for DAPI imaging or VVG staining. For DAPI staining of cell nuclei, 3 μL (5 mg/mL) of diluted DAPI was added to the samples in 1 mL of PBS (pH 7.4). The VVG staining procedure followed a protocol published by the American Society of Clinical Pathologists.[48] Verhoeff's solution was prepared by mixing 30 mL of hematoxylin (Gill's no. 3), 12 mL of 10% (m/v) ferric chloride, and 12 mL of Lugol's iodine. Gill's no. 3 turns the elastic lamina brown. The Verhoeff solution that was used produced a brown color change specific to elastin-containing matrixes. Tissue sections were placed into Verhoeff's solution for 1 h, and then rinsed twice with deionized water. Sections were then differentiated in a 2% (m/v) ferric chloride solution. The sections were again rinsed with distilled water, treated with 5% (m/v) sodium thiosulfate for 1 min, and rinsed in tap water three times. Sections were counterstained in Van Gieson's solution for 30 s, differentiated in 95% alcohol, dehydrated with absolute ethanol, and cleared in xylene substitute before mounting and imaging.

Explanted samples were additionally stained by H&E. Ethanol-fixed cross-sections were washed in three changes of PBS (pH 7.4) for 5 min each, followed by a wash in deionized water for 5 min. The samples were then placed in Gill's no. 3 for 5 min to fully stain the sections. The slides were then differentiated by dipping five times into a solution of hydrochloric acid in deionized water (pH 2). Once differentiated, the slides were placed into deionized water for 1 min to blue them. The blued samples were placed into two changes of 95% ethanol for 5 min per change. Eosin Y (0.25%) was then used to counterstain the sections for 30 s, after which they were dehydrated in absolute ethanol and cleared in xylene substitute. The samples were then mounted and imaged.

3. RESULTS

3.1. Decellularization and Stabilization of Elastic Lamina. Histological analysis of the processed aortic specimens demonstrated successful isolation of the elastic lamina. The elastic lamina was clearly defined (shown as brown fibers) with no collagen-bearing matrixes observed between the layers of elastic lamina or inner/outer vascular layers (Figure 1A,B).

DOI: 10.1021/acsami.5b03892
ACS Appl. Mater. Interfaces 2015, 7, 16202–16212

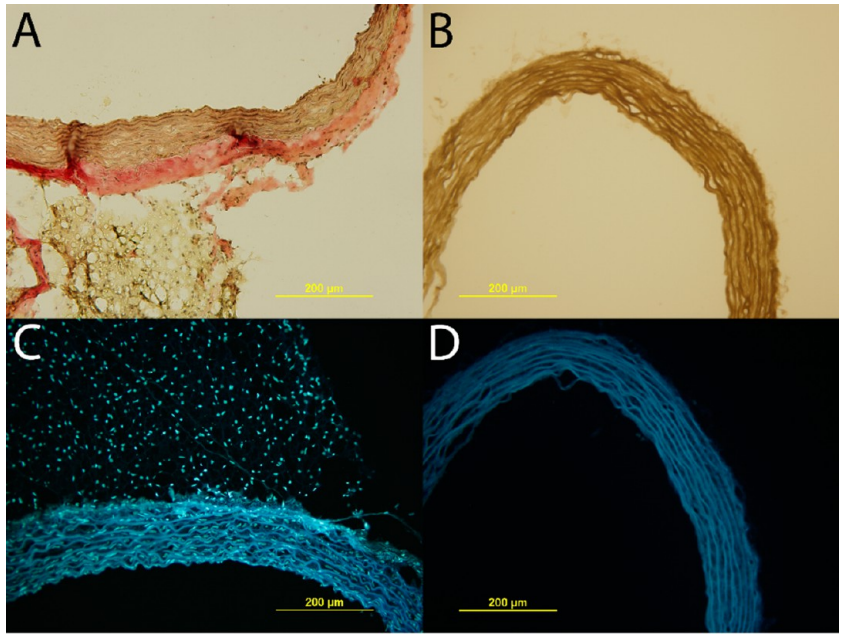

Figure 1. Representative images for native and decellularized/decollagenized arterial cross-sections. (A, B) Elastic lamina stained with VVG to show collagens present in the unprocessed vessel (A) and their absence in the processed tissue (B). (C, D) Cell nuclei were stained with DAPI to show cellularization of the elastic lamina and adventitial layers of the native artery (C) and the absence of cell nuclei after decellularization (D). The blue fibers in (C) and (D) are due to inherent fluorescence from the elastic lamina, not from DAPI staining.

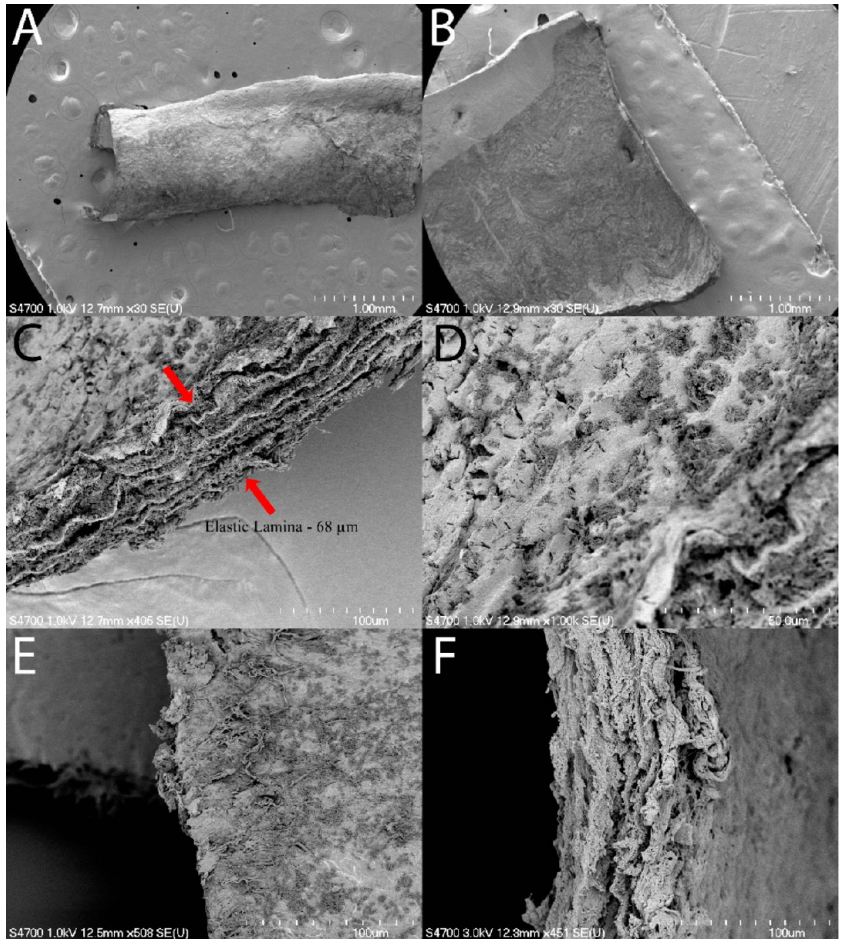

Figure 2. SEM images of the decellularized elastin scaffold. (A) External view. (B) Internal view. (C) Internal surface/scaffold wall. (D) Magnified image of the internal surface from window C. (E) Magnified image of the external surface and scaffold edge. (F) Magnified image of the external surface/scaffold wall.

DOI: 10.1021/acsami.5b03892
ACS Appl. Mater. Interfaces 2015, 7, 16202−16212

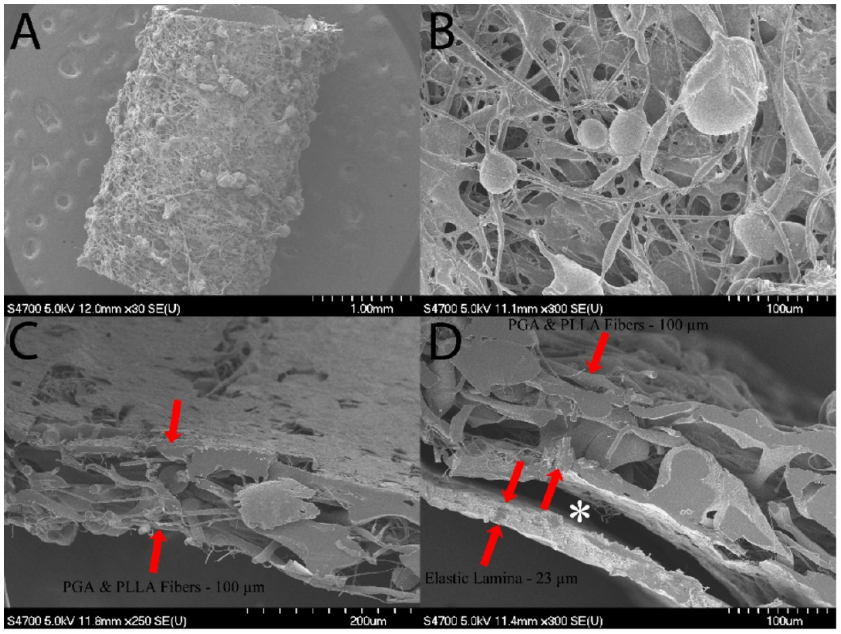

Figure 3. SEM images showing the fiber morphology of the PGA/PLLA vascular graft. (A) Wide view of the intact graft. (B) Magnified view of the graft. (C) Image of the elastic lamina contacting side of the fiber layer without the elastic lamina. (D) Edge view of the assembled graft with polymer layers and the elastic lamina. Asterisks denote delamination due to the FESEM preparation protocol. $n = 2$.

The processed specimens were found to be completely devoid of cell nuclei (Figure 1C,D). Success of the decellularization processing was further confirmed by electron microscopy. FESEM images of the processed elastic lamina depict an intact elastic lamina matrix composed of several layers, with interconnecting fibers (Figure 2). The internal surface of the elastic lamina is irregular, with many crevices. The thickness of the elastic lamina varied between 40 and 80 μm.

Elastic lamina matrixes that were UV-treated for 2 h exhibited more favorable mechanical properties relative to the nontreated matrixes. After treatment, the decellularized elastin vessels were able to support themselves partially open.

3.2. Aortic Engraftment Using Only UV-Treated Elastic Lamina. After determination that UV treatment for 2 h improved the material handling properties and mechanical strength, an early attempt was made to engraft a segment into the rat abdominal aorta, without polymeric support. Unfortunately, as the sutures were placed and tightened, tears appeared in the elastic lamina scaffold (data not shown). This result suggested the treatment decreased the elastic lamina's resistance to tearing.

3.3. Early Hybrid Grafts. This early engraftment demonstrated the need for external mechanical support of the elastin matrix via polymer coating. To accomplish this, a spray-coated layer of PGA in HFIP was deposited on the external elastic lamina surface. PGA acted as a transitional layer to connect an electrospun PLLA scaffold to the elastic lamina, while improving the graft's mechanical properties. Once dried, PLLA electrospun fibers were deposited over the PGA surface. These fibers were found to be unaligned. The fibers were found to have widely varying diameters and orientations, which promotes suturability and mechanical isotropy in the electrospun fiber layer. The innermost fiber layer contained relatively small diameter fibers with few defects. The outermost layer generally contained larger diameter fibers, with significant necking and branching, indicative of poor grounding of the mandrel due to fiber buildup. Pore sizes between the fibers appeared to vary on the basis of the layer in which they were deposited (Figure 3A–C). Large pores between fibers are anticipated to permit cellular infiltration.

An FESEM image of the fabricated construct demonstrated sufficient adhesion to promote graft stability between the deposited PGA layer and the PLLA fibers, even after several cycles of hydration and dehydration (Figure 3C). It is important to note that the FESEM sample preparation caused slight delamination of the PGA layer from the elastic lamina surface due to the requisite dehydration (Figure 3D). This effect was not observed during processing or surgery, but suggests the adhesion between these layers could be improved. Despite this shortcoming, the overall mechanical integrity of the hybrid construct was much preferable relative to that of the UV-treated elastic lamina.

3.4. Aortic Engraftment of PGA/PLLA Hybrid Constructs. After observation of good suturability and layer adhesion, the PGA/PLLA/elastic lamina constructs were interposed and sutured into the rat abdominal aorta. The luminal elastic lamina surface of a representative graft prior to implantation is shown in Figure S2A,B (Supporting Information). The graft was collected for analysis after either 1 h (Figure S2C,D) or 3 days (Figure S3, Supporting Information) postimplantation ($n = 1$ per time point). The 1 h sample was free from obvious signs of blood coagulation. The 3 day vessel also showed no obvious signs of blood coagulation. Staining confirmed the absence of cellular infiltrates into the elastic lamina matrix (Figure S3C–G). A comparison between the 3 day graft and the native artery at the graft/artery interface demonstrates the absence of cell nuclei in the fabricated grafts as compared to the native artery, as well as the continuous surface of the elastic lamina up to the endothelialized host artery (Figure S3G,H). There was evidence of modest blood coagulation at the suture line, which is attributable to blood contact with either the suture material or PGA/PLLA that became exposed during suturing.

DOI: 10.1021/acsami.5b03892
ACS Appl. Mater. Interfaces 2015, 7, 16202–16212

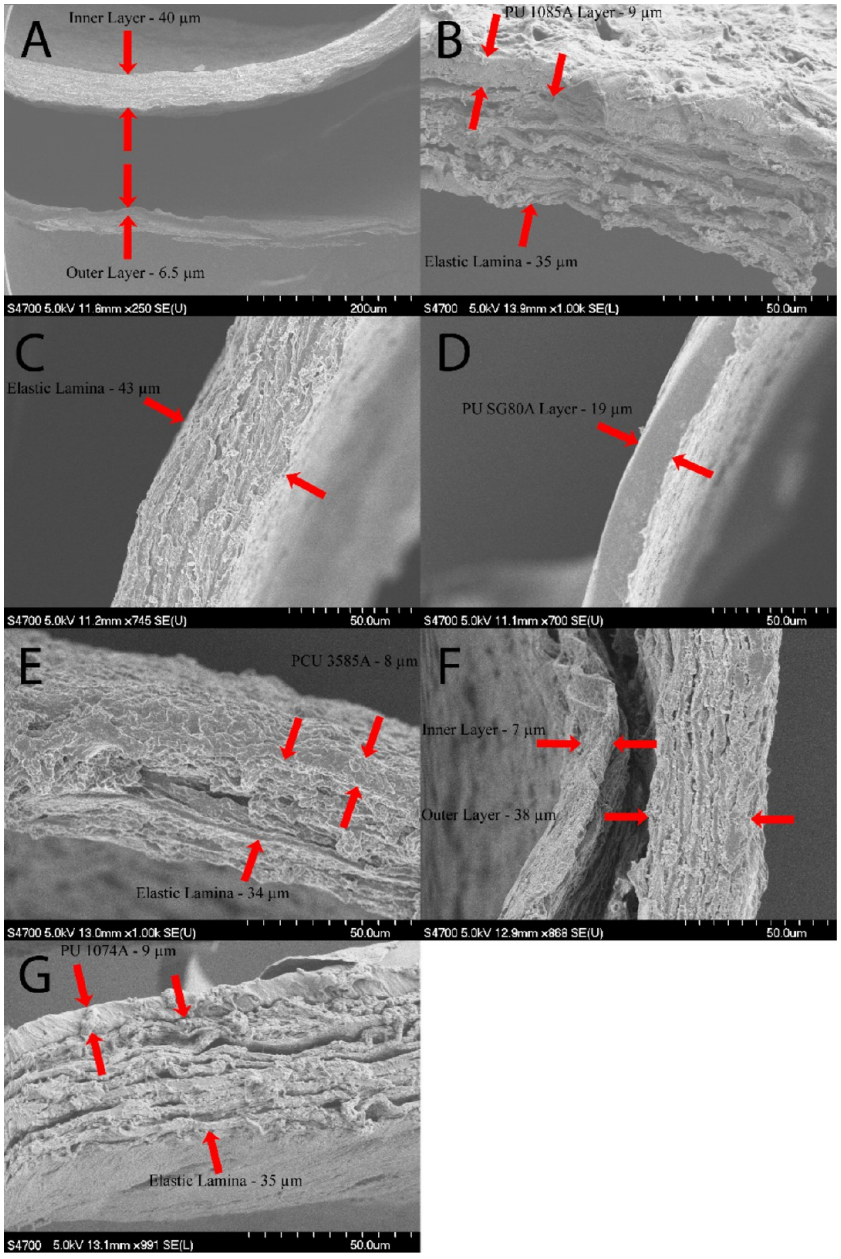

Figure 4. High-magnification FESEM images of the polymer/elastic lamina interface for (A) PCL, (B) PEU 1085A, (C, D) PEU SG80A, (E) PCU 3585A, (F) PCU 4085A, and (G) PEU 1074A. The thickness of each layer is labeled in each panel. n = 2 per polymer coating.

Although the PGA/PLLA/elastic lamina graft performed well overall, the graft was found to be excessively brittle, as the PLLA layer cracked and flaked to some extent during suturing. Furthermore, adhesion defects revealed by SEM processing (Figure 3D) suggested that the PGA layer was not able to strongly adhere to the elastic lamina. For this reason, it was necessary to explore other polymeric biomaterials that could better serve as mechanical reinforcement to the elastic lamina.

3.5. Fabrication and Performance of Improved Hybrid Grafts. Polymer selection to identify materials with superior performance began by identifying well-characterized polymers with lower crystallinity and higher elastic moduli relative to PGA and PLLA. Table 1 lists the relevant properties of the considered materials. Most of the selected materials were hydrophobic to some degree, and all possessed high elongations to failure (≥400%). The hydrophobicity of some materials was anticipated to assist in adhesion to the hydrophobic elastic lamina. High elongations to failure implied that these materials were less likely to crack during processing and surgical implantation.

Polymer-coated samples were examined for delamination after hydration in PBS (Figure S4, Supporting Information). Both PCL and PEU SG80A suffered from severe delamination and were therefore eliminated from consideration. Further delamination analysis was performed by dehydrating the hybrid grafts and examining an example of each in cross-section (Figure S5, Supporting Information). Again, PCL and PEU SG80A scaffolds were found to adhere poorly to the elastic lamina. Minor delamination was also seen with PCU 4085A. Magnified images of the scaffolds were collected for closer inspection of the polymer/elastic lamina interface (Figure 4). PCL was completely delaminated from the elastic lamina layer.

DOI: 10.1021/acsami.5b03892
ACS Appl. Mater. Interfaces 2015, 7, 16202−16212

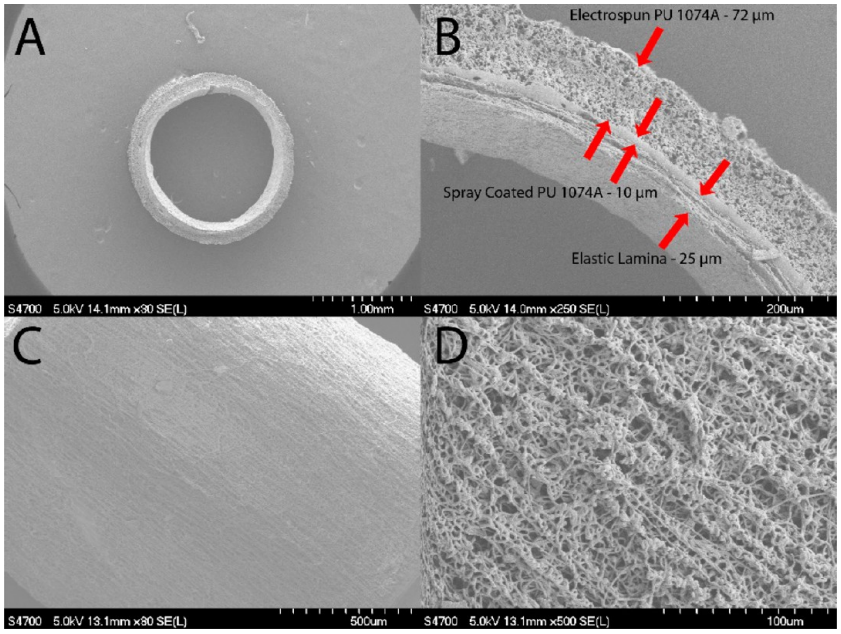

Figure 5. Elastic lamina coated in PEU 1074A with electrospun PEU 1074A fibers deposited externally. (A, B) Cross-sectional view of the preimplantation specimen, demonstrating good adhesion between the layers. (C, D) Longitudinal view of the preimplantation specimen's fibers, showing unexpected partial longitudinal fiber alignment. Both polymers were dissolved in HFIP for coating. n = 2.

PEU 1085A exhibited adequate adhesion between the polymer/elastin layers. PEU SG80A was completely delaminated (elastic lamina shown in Figure 4C and separated polymer coating shown in Figure 4D). PCU 3585A was well adhered to the elastic lamina. In this case, the polymer layer was difficult to distinguish from the elastin. PCU 4085A was delaminated in several areas of the sample. Due to this result, PCU 4085A was eliminated from further evaluation. PEU 1074A was found to have excellent adhesion to the elastic lamina matrix.

The successful polymers (PEU 1074A, PEU 1085A, and PCU 3585A) were then evaluated in a suture pullout test to provide information on how they would perform during suturing. The elastic lamina was spray coated with the three remaining polymers and electrospun with PLLA fibers and underwent a suture pullout event followed by FESEM imaging of the failure surfaces (data not shown). An ideal suture pullout should reveal good elasticity and plastic deformation, but also good resistance to suture pullout. PEU 1074A resisted suture pullout without exhibiting brittle fracture. PEU 1085A failed with low resistance and was consequently dismissed from consideration. PCU 3585A failed by brittle fracture and was also removed from further consideration. Therefore, PEU 1074A was deemed the best material of those considered for this application.

3.6. Poly(ether urethane) (PEU 1074A) Hybrid Graft Implantation. Prior to implantation, the PEU 1074A/elastic lamina conduit was further improved by electrospinning fibers using PEU 1074A dissolved in HFIP (Figure 5) in place of the electrospun PLLA fibers used in previous tests. This modification was found to vastly improve the interfacial adhesion between the polymer layers, and also resulted in better quality fibers in the fully assembled vascular graft. After 3 days postimplantation (n = 1), the graft was excised and characterized histologically (Figure S6, Supporting Information). A longitudinal cut made to expose the luminal graft surface revealed a small region with attached coagulated blood. This material was loosely adhered to the suture line at the distal end of the graft but was not attached to the elastic lamina surface. An H&E stain showed significant cellular infiltration into the electrospun PEU 1074A fibers, as well as a thin thrombus layer near the suture site. The thrombus layer thickness was well below 10 μm at most locations away from the suture line. After 21 days postimplantation (n = 5), the grafts were excised and characterized (Figure 6). All five grafts were patent, with clear signs of arterial pulsation evident at both distal and proximal host locations. H&E stains verified patent lumens as well as the formation of a relatively thin neointima on the luminal surface of the grafts (Figure 6B). Some wrinkling of the elastic lamina and artificial detachment of the polymer coating due to cross-sectioning is evident. Typical low (Figure 6C) and high (Figure 6D) neointimal tissue thicknesses are shown. Delamination of the polymer coating from the elastic lamina was commonly detected post-cross-sectioning (Figure 6B,D). However, delamination is unlikely to have been a dominant factor in situ, as excellent interfacial adhesion was seen at the sites of pores within the elastic lamina (Figure 6E). These sites provide direct contact between the polymer and blood flow/pressure and are therefore natural nucleation sites for delamination, if it were to occur. In rare cases, cells could be seen residing within the elastic lamina (Figure 6D). Sites of wrinkling (Figure 6B) and pores (Figure 6E) were associated with an increased neointimal thickness.

3.7. Mechanical Evaluation of Hybrid Vascular Grafts. Characterization of the electrospun PEU 1074A fibers and mechanical properties of the graft are shown in Table 2. We found burst pressures to be well in excess of physiological demands and in accordance with other experimental vascular grafts.[49−51] In one specimen, the elastic lamina was seen to delaminate from the reinforcing polymer at ∼800 mmHg, prior to burst failure of the polymer layer. Notably, the elastic lamina did not delaminate from any of the other specimens, despite the presence of large pores in this layer due to extensive arterial side-branching at the donor site. Thus, the elastic lamina and polymer layers exhibited excellent interfacial adhesion.

DOI: 10.1021/acsami.5b03892
ACS Appl. Mater. Interfaces 2015, 7, 16202−16212

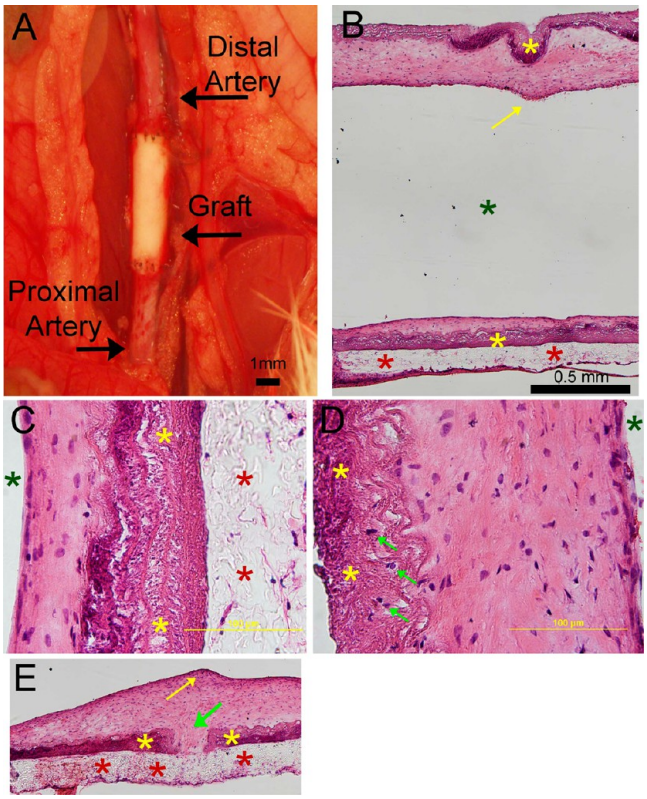

Figure 6. Characterization of the 21 day PEU 1074A vascular graft. (A) The PEU 1074A graft is shown prior to collection. (B) H&E staining of a vessel transverse section demonstrates modest neointimal formation on both sides of the graft (top and bottom of the image) and an open lumen. (C) Magnified view of a representative low-thickness neointimal layer. Polymer coating can be seen adhering to the elastic lamina. (D) Magnified view of a representative high-thickness neointimal layer. Cell nuclei can be seen to have migrated into the elastic lamina. Dark green stars identify the lumen, red stars identify the polymer, and yellow stars identify the elastic lamina. Light green arrows identify cells within the elastic lamina in (D). The light green arrow in (E) identifies a pore in the elastic lamina, which is created by arterial side branching at the donor site. Yellow arrows in (B) and (E) identify protrusion of the neointimal layer into the lumen due to elastic lamina defects. Blood flow proceeds from left to right in (B) and (E). The scale bar for (E) is the same as that shown in (B).

Due to the negligible contributions of both the elastic lamina and spray-coated layer to the mechanical properties of the vessel, tensile testing was restricted to the two different electrospun fibers used to construct all of the hybrid vascular grafts. A representative stress−strain plot for both the electrospun PLLA and PEU 1074A fibers can be seen in Figure S7 (Supporting Information). While the relatively brittle character of the PLLA fibers allowed all samples to be evaluated to failure, the exceptional elasticity of the PEU 1074A fibers prevented the collection of failure data for this material. The average elastic modulus of the electrospun fibers was 64 ± 35 MPa for the PLLA samples and 1.4 ± 0.8 MPa for the PEU 1074A samples. The elongation to failure for PLLA was 10.1 ± 4.1%. The average observed elongation of the PEU 1074A without failure was 195 ± 24%. These data are summarized in Table S8 (Supporting Information).

4. DISCUSSION

Here, we have constructed a novel vascular graft by supporting an elastic lamina blood-contacting surface with polymeric materials. The graft was easy to manipulate and suture. Importantly, the graft avoided significant inflammatory responses and progressive intimal hyperplasia, both widely recognized as mediating factors in restenosis. The elastic lamina appears to exert suppressive effects on resident cells. This requires receptor-mediated signaling mechanisms, which employ a ligand with precise protein structure and electrostatic activity.[15] Thus, it seems that the processing conditions used to construct the graft (e.g., NaOH decellularization, UV irradiation, and ethylene oxide treatments) did not substantially alter the chemical composition of the elastic lamina.

An ideal vascular graft should match the mechanical characteristics of the native artery. Concurrently, viable vascular grafts must mimic the properties of a native endothelium at the blood-contacting surface, not provoke an inflammatory response, remain shelf-stable over extended time periods prior to use, and be easy to handle and suture. The latter requirement precludes the presence of cellular fragments or DNA from the donor. It has been challenging thus far for the scientific and industrial community to develop a graft that possesses all of these ideal properties. This is mainly due to the challenge of mimicking a confluent endothelium on the luminal surface of acellular materials and the difficulties in generating universally compatible implant materials from cellularized constructs.

The grafts developed here have a wall thickness and burst pressure similar to those of the native saphenous vein, which is a widely used autologous conduit for coronary artery bypass grafting. Specifically, the native saphenous vein has a burst pressure of 1600−2500 mmHg and a wall thickness of 250 μm.[52] While the present vascular grafts exhibit a slightly lower average burst pressure of 990 ± 112 mmHg, their wall thickness is less than half that of the saphenous vein at 106 ± 42 μm. These data would suggest a similar mechanical strength for the bulk material.

Tensile evaluation of the PLLA and PEU 1074A electrospun polymers revealed a clear difference in their mechanical properties as the brittle behavior of the PLLA was evident. The relative brittleness of PLLA is consistent with tabulated mechanical data presented in Table 1, which lists PLLA as having among the lowest elongations to failure. In contrast, the final polymer used in this work, PEU 1074A, exhibited exceptional elastic behavior in both burst pressure and tensile tests. Ideally, the selected reinforcing polymer for the vascular graft should possess mechanical properties similar to those of

Table 2. Summary of the Physical Properties of the Vessels[a]

	wall thickness (μm)	burst pressure (mmHg)	fiber diameter (μm)	fiber density (no. of fibers/mm)
PEU-coated elastin vascular grafts	N/A	197 ± 29	N/A	N/A
	106 ± 42	990. ± 112	1.68 ± 0.66	204 ± 80

[a]Values are reported with standard deviations. n = 4 for burst pressure and wall thickness measurements. n = 3 for fiber diameter and density measurements. N/A means not applicable.

DOI: 10.1021/acsami.5b03892
ACS Appl. Mater. Interfaces 2015, 7, 16202−16212

native blood vessels. The elastic modulus of a typical, nondiseased human coronary artery is 1.48 MPa,[53] while the elongation to failure of the human carotid artery is reported as 105%.[20] Thus, the mechanical properties of a native small-diameter human artery are similar to those of PEU 1074A.

In the case of the present hybrid graft, the main function of the polymeric biomaterials (either the biodegradable PLLA or biostable PEU 1074A) is to provide mechanical support. In this role, polymeric supporting materials can be optimized with fewer concerns for blood-contacting properties, and allow development to move toward matching their mechanical characteristics to the native artery. Meanwhile, the elastic lamina provides an excellent acellular blood-contacting layer, which has been a serious limitation of acellular materials to date. Conversely to the polymer materials, the elastic lamina may be harvested and processed with little concern for its mechanical performance. Thus, the multilayered design of the present engineered acellular vascular graft, with a biological layer and a synthetic layer that are each optimized for different functions, makes it more feasible to achieve the overall performance goals. Such a graft, because it is acellular, can be developed specifically as a xenograft from the artery of any donor animal and be implanted into any recipient. It is also shelf-stable and can be quickly hydrated in the operating room, and therefore can be stocked to meet the urgent needs of surgeons and patients.

During the course of evaluation, a number of defects in these experimental grafts became evident. These included rare cases of cell migration into the elastic lamina and regions of delamination between the different polymers and elastic lamina. Although we have achieved excellent results with the present processing conditions, the processing steps are amenable to improvements. Further refinement may result in a reduced neointimal tissue development relative to what was found here. For example, alternative techniques to decellularize and purify the elastic lamina could be employed to better preserve the structural and chemical integrity of its constituent proteins, which serve as ligands for the receptor-mediated signaling events that suppress cellular activity. The presence of cells within the elastic lamina at rare sites in the 21 day grafts suggests that processing conditions may have locally altered the chemical structure of the elastic lamina. Altering the molecular weight or solvent concentration in polymer processing may improve adhesion between the PLLA and elastic lamina and provide a testable, biodegradable graft to compare at longer times with the biostable PEU 1074A graft. In addition, consistency between batches of vascular grafts would benefit from more automated and controlled processing and fabrication conditions.

While characterizing the hybrid grafts, we observed longitudinal alignment of electrospun fibers in the PEU 1074A graft. This fiber orientation will cause the material to be resilient when stretched along the longitudinal direction, but may create deficiencies in resisting large hoop stresses. While this introduces some concerns, the grafts were still able to resist arterial pulsatile pressure and retain sutures for up to 21 days. Future work with this material will aim to provide a more uniform distribution of fiber alignment with the ultimate goal of achieving mechanical isotropy in the structural coating.

It is important to note that the low degree of thrombus formation in the elastic lamina/PEU 1074A graft was similar to that of the elastic lamina/PGA/PLLA graft at the 3 day time point. This is likely due to the excellent hemocompatibility of the elastic lamina, and confirms that the hybrid conduit design offers flexibility in polymer selection. Surprisingly, although the PLLA electrospun fiber layer was thicker than that of the PEU 1074A fibers, there was markedly more cellular infiltration seen within the PEU 1074A fibers. This is likely due to a combination of differences in porosity, pore size distribution, fiber diameter, hydrophobicity/hydrophilicity, and the associated degree of swelling between the two constructs. Because cellular infiltration into the graft is necessary for integration of the material, the ability of cells to infiltrate and the type of cell infiltrates represent an additional consideration for polymer selection and modification, especially if biodegradable constructs are being considered.

Future work aimed at improving the performance of the vascular graft could be directed toward clarifying the key factors that regulate interfacial adhesion between the polymer and elastic lamina. Such an assessment may reduce the reliance upon bulk properties for material selection. Future experiments with longer term in vivo implantations (between 6 months and 1 year) will enable a more thorough characterization of the long-term biocompatibility of the graft. Lastly, optimization of the donor artery processing conditions may reduce chemical and physical alterations of the elastic lamina from its native state and better preserve the cell suppressive properties that make this material an excellent blood-contacting layer.

5. CONCLUSION

This work has demonstrated an effective approach for the construction of hybrid vascular grafts with natural elastic lamina as blood-contacting surfaces. Using simple tissue engineering techniques and fabrication methods, a vascular construct has been devised that demonstrates promising short-term performance as a vascular graft, in vivo. The vessel fabricated in this work improves upon current small-diameter vascular grafts by making use of an elastic lamina blood-contacting layer, which has been shown to be nonthrombogenic, nonimmunogenic, and neointimal hyperplasia resistant. As compared to experimental vascular grafts that rely upon synthetic elastin or elastin-like polypeptides, our approach decellularizes widely available donor tissue. The arteries of larger animals could serve as donors for human applications. This approach minimizes the costs, simplifies the fabrication process, and preserves the native architecture and biological properties of the elastic lamina. The use of synthetic polymers to provide mechanical reinforcement is another innovative feature that allows for extensive refinement of the mechanical properties in the final product. Further innovation may involve the incorporation of drug-releasing components into the polymeric material.

The positive results of this work open the door for further development of the decellularization methods, polymers, coating techniques, and electrospinning process. A shelf-stable vascular graft containing a natural and intact elastic lamina that reduces the natural tendency of the host environment to respond to vascular engraftment with platelet activation, excessive thrombogenesis, and intimal hyperplasia may provide a new direction for developing small-diameter vascular grafts, particularly for coronary artery bypass procedures.

■ ASSOCIATED CONTENT

Supporting Information

Additional information on the initial development and short-term testing of the vascular graft described in the text. The

DOI: 10.1021/acsami.5b03892
ACS Appl. Mater. Interfaces 2015, 7, 16202−16212

Supporting Information is available free of charge on the ACS Publications website at DOI: 10.1021/acsami.5b03892.

AUTHOR INFORMATION

Corresponding Author

*Phone: 906-487-2851. Fax: 906-487-1717. E-mail: jgoldman@mtu.edu.

Notes

The authors declare no competing financial interest.

ACKNOWLEDGMENTS

This work was supported by National Institutes of Health Contract Grant R15-HL-113954 (the contract grant sponsors were Jon Stinson and Peter Edelman, Boston Scientific Corp.). F.Z. was supported by NIH Grant 1R15HL115521-01A1. P.K.B. was supported by an American Heart Association predoctoral fellowship. The authors would like to thank David Rosen for his assistance with the Bose Electroforce 3200.

REFERENCES

(1) Nottelet, B.; Pektok, E.; Mandracchia, D.; Tille, J.; Walpoth, B.; Gurny, R.; Möller, M. Factorial Design Optimization and *In Vivo* Feasibility of poly(e-caprolactone)-micro- and Nanofiber-Based Small Diameter Vascular Grafts. *J. Biomed. Mater. Res., Part A* **2009**, *89A*, 865−875.

(2) Wang, X.; Lin, P.; Yao, Q.; Chen, C. Development of Small-Diameter Vascular Grafts. *World J. Surg.* **2007**, *31*, 682−689.

(3) Kannan, R.; Salacinski, H.; Butler, P.; Hamilton, G.; Seifalian, A. Current Status of Prosthetic Bypass Grafts, A Review. *J. Biomed. Mater. Res., Part B* **2005**, *74B*, 570−581.

(4) Nerem, R.; Seliktar, D. Vascular Tissue Engineering. *Annu. Rev. Biomed. Eng.* **2001**, *3*, 225−243.

(5) Desai, M.; Seifalian, A.; Hamilton, G. Role of Prosthetic Conduits in Coronary Artery Bypass Grafting. *Eur. J. Cardiothorac. Surg.* **2011**, *40*, 394−398.

(6) Wu, H.; Fan, J.; Chu, C.; Wu, J. Electrospinning of Small Diameter 3-D Nanofibrous Tubular Scaffolds with Controllable Nanofiber Orientations for Vascular Grafts. *J. Mater. Sci.: Mater. Med.* **2010**, *21*, 3207−3215.

(7) De Visscher, G.; Mesure, L.; Meuris, B.; Ivanova, A.; Flameng, W. Improved Endothelialization and Reduced Thrombosis by Coating a Synthetic Vascular Graft with Fibronectin and Stem Cell Homing Factor SDF-1α. *Acta Biomater.* **2012**, *8*, 1330−1338.

(8) Hashi, C.; Derugin, N.; Janairo, R.; Lee, R.; Schultz, D.; Lotz, J.; Li, S. Antithrombogenic Modification of Small-Diameter Microfibrous Vascular Grafts. *Arterioscler., Thromb., Vasc. Biol.* **2010**, *30*, 1621−1627.

(9) Avci-Adali, M.; Ziemer, G.; Wendel, H. Induction of EPC Homing on Biofunctionalized Vascular Grafts for Rapid *In Vivo* Self-Endothelialization — A Review of Current Strategies. *Biotechnol. Adv.* **2010**, *28*, 119−129.

(10) Novosel, E.; Kleinhans, C.; Kluger, P. Vascularization is the Key Challenge in Vascular Tissue Engineering. *Adv. Drug Delivery Rev.* **2011**, *63*, 300−311.

(11) Naito, Y.; Shinoka, T.; Duncan, D.; Hibino, N.; Solomon, D.; Cleary, M.; Rathore, A.; Fein, C.; Church, S.; Breuer, C. Vascular Tissue Engineering, Toward the Next Generation Vascular Grafts. *Adv. Drug Delivery Rev.* **2011**, *63*, 312−323.

(12) Nieponice, A.; Soletti, L.; Guan, J.; Hong, Y.; Gharaibeh, B.; Maul, T.; Huard, J.; Wagner, W.; Vorp, D. *In Vivo* Assessment of a Tissue-Engineered Vascular Graft Combining a Biodegradable Elastomeric Scaffold and Muscle-Derived Stem Cells in a Rat Model. *Tissue Eng., Part A* **2010**, *16*, 1215−1223.

(13) Uttayarat, P.; Perets, A.; Li, M.; Pimton, P.; Stachelek, S.; Alferiev, I.; Composto, R.; Levy, R.; Lelkes, P. Micropatterning of Three-Dimensional Electrospun Polyurethane Vascular Grafts. *Acta Biomater.* **2010**, *6*, 4229−4237.

(14) Liu, S.; Tieche, C.; Alkema, P. Neointima Formation on Vascular Elastic Laminae and Collagen Matrices Scaffolds Implanted in the Rat Aortae. *Biomaterials* **2004**, *25*, 1869−1882.

(15) Liu, S.; Alkema, P.; Tieché, C.; Tefft, B.; Liu, D.; Li, Y.; Sumpio, B.; Caprini, J.; Paniagua, M. Negative Regulation of Monocyte Adhesion to Arterial Elastic Laminae by Signal Regulatory Protein and Src Homology 2 Domain-containing Protein-Tyrosine Phosphatase-1*. *J. Biol. Chem.* **2005**, *280*, 39294−39301.

(16) Hinds, M.; Rowe, R.; Ren, Z.; Teach, J.; Wu, P.; Kirkpatrick, S.; Breneman, K.; Gregory, K.; Courtman, D. Development of a Reinforced Porcine Elastin Composite Vascular Scaffold. *J. Biomed. Mater. Res., Part A* **2006**, *77A*, 458−469.

(17) Simionescu, D.; Lu, Q.; Song, Y.; Lee, J.; Rosenbalm, T.; Kelley, C.; Vyavahare, N. Biocompatibility and Remodeling Potential of Pure Arterial Collagen and Elastin Scaffolds. *Biomaterials* **2006**, *27*, 702−713.

(18) Blit, P.; McClung, W.; Brash, J.; Woodhouse, K.; Santerre, J. Platelet Inhibition and Endothelial Cell Adhesion on Elastin-Like Polypeptide Surface Modified Materials. *Biomaterials* **2011**, *32*, 5790−5800.

(19) Srokowski, E.; Woodhouse, K. Surface and Adsorption Characteristics of Three Elastin-Like Polypeptide Coatings with Varying Sequence Lengths. *J. Mater. Sci.: Mater. Med.* **2013**, *24*, 71−84.

(20) McKenna, K.; Hinds, M.; Sarao, R.; Wu, P.; Maslen, C.; Glanville, R.; Babcock, D.; Gregory, K. Mechanical Property Characterization of Electrospun Recombinant Human Tropoelastin for Vascular Graft Biomaterials. *Acta Biomater.* **2012**, *8*, 225−233.

(21) Waterhouse, A.; Wise, S.; Ng, M.; Weiss, A. Elastin as a Nonthrombogenic Biomaterial. *Tissue Eng., Part B* **2011**, *17*, 93−99.

(22) Wise, S.; Byrom, M.; Waterhouse, A.; Bannon, P.; Ng, M.; Weiss, A. A Multilayered Synthetic Human Elastin/Polycaprolactone Hybrid Vascular Graft with Tailored Mechanical Properties. *Acta Biomater.* **2011**, *7*, 295−303.

(23) McClure, M.; Simpson, D.; Bowlin, G. Tri-layered Vascular Grafts Composed of Polycaprolactone, Elastin, Collagen, and Silk: Optimization of Graft Properties. *J. Mech. Behav. Biomed. Mater.* **2012**, *10*, 48−61.

(24) Cheung, H.; Lau, K.; Lu, T.; Hui, D. A Critical Review on Polymer-Based Bio-engineered Materials for Scaffold Development. *Composites, Part B* **2007**, *38*, 291−300.

(25) Guo, B.; Ma, P. X. Synthetic Biodegradable Functional Polymers for Tissue Engineering, A Brief Review. *Sci. China: Chem.* **2014**, *57*, 490−500.

(26) Dhandayuthapani, B.; Yoshida, Y.; Maekawa, T.; Kumar, D. Polymeric Scaffolds in Tissue Engineering Application, A Review. *Int. J. Polym. Sci.* **2011**, *2011*, 1−20.

(27) Lasprilla, A.; Martinez, G.; Lunelli, B.; Jardini, A.; Filho, R. Poly-lactic Acid Synthesis for Application in Biomedical Devices — A Review. *Biotechnol. Adv.* **2012**, *30*, 321−328.

(28) Maurus, P.; Kaeding, C. Bioabsorbable Implant Material Review. *Oper. Techn. Sport Med.* **2004**, *12*, 158−160.

(29) Oksman, K.; Skrifvars, M.; Selin, J. Natural Fibres as Reinforcement in Polylactic Acid (PLA) Composites. *Compos. Sci. Technol.* **2003**, *63*, 1317−1324.

(30) Plackett, D.; Andersen, T. L.; Pedersen, W. B.; Nielsen, L. Biodegradable Composites Based on L-polylactide and Jute Fibres. *Compos. Sci. Technol.* **2003**, *63*, 1287−1296.

(31) Ma, Z.; Gao, C.; Gong, Y.; Shen, J. Chondrocyte Behaviors on Poly-l-lactic Acid (PLLA) Membranes Containing Hydroxyl; Amide or Carboxyl Groups. *Biomaterials* **2003**, *24*, 3725−3730.

(32) Vieira, A.; Vieira, J.; Guedes, R.; Marques, A. Experimental Degradation Characterization of PLA-PCL; PGA-PCL; PDO; and PGA Fibres. *ICCM Proc. Int. Conf. Compos. Mater.* **2009**, *7*, 27−31.

(33) Yoon, J.; Jung, H.; Kim, M.; Park, E. Diffusion Coefficient and Equilibrium Solubility of Water Molecules in Biodegradable Polymers. *J. Appl. Polym. Sci.* **2000**, *77*, 1716−1722.

(34) Matzinos, P.; Tserki, V.; Kontoyiannis, A.; Panayiotou, P. Processing and Characterization of Starch/Polycaprolactone Products. *Polym. Degrad. Stab.* **2002**, *77*, 17−24.

(35) Yang, M.; Zhang, Z.; Hahn, C.; Laroche, G.; King, M.; Guidoin, R. Totally Implantable Artificial Hearts and Left Ventricular Assist Devices: Selecting Impermeable Polycarbonate Urethane to Manufacture Ventricles. *J. Biomed. Mater. Res.* **1999**, *48*, 13−23.
(36) Marletta, G.; Ciapetti, G.; Satriano, C.; Pagani, S.; Baldini, N. The Effect of Irradiation Modification and RGD Sequence Adsorption on the Response of Human Osteoblasts to Polycaprolactone. *Biomaterials* **2005**, *26*, 4793−4804.
(37) Chen, R.; Huang, C.; Ke, Q.; He, C.; Wang, H.; Mo, X. Preparation and Characterization of Coaxial Electrospun Thermoplastic Polyurethane/Collagen Compound Nanofibers for Tissue Engineering Applications. *Colloids Surf., B* **2010**, *79*, 315−325.
(38) Goldman, J.; Zhong, L.; Liu, S. Negative Regulation of Vascular Smooth Muscle Cell Migration by Blood Shear Stress. *Am. J. Physiol.* **2007**, *292*, H928−H938.
(39) Gunatillake, P.; Adhikari, R. Biodegradable Synthetic Polymers for Tissue Engineering. *Eur. Cells Mater.* **2003**, *5*, 1−16.
(40) Labet, M.; Thielemans, W. Synthesis of Polycaprolactone, a Review. *Chem. Soc. Rev.* **2009**, *38*, 3484−3504.
(41) Williamson, M.; Black, R.; Kielty, C. PCL-PU Composite Vascular Scaffold Production for Vascular Tissue Engineering; Attachment; Proliferation and Bioactivity of Human Vascular Endothelial Cells. *Biomaterials* **2006**, *27*, 2608−2616.
(42) Tanzi, M.; Mantovani, D.; Petrini, P.; Guidoin, R.; Laroche, G. Chemical Stability of Polyether Urethanes Versus Polycarbonate Urethanes. *J. Biomed. Mater. Res.* **1997**, *36*, 550−559.
(43) Guo, J.; Feng, Y.; Ye, Y.; Zhao, H. Construction of Hemocompatible Polycarbonate Urethane with Sulfoammonium Zwitterionic Polyethylene Glycol. *J. Appl. Polym. Sci.* **2011**, *122*, 1084−1091.
(44) Tatai, L.; Moore, T.; Adhikari, R.; Malherbe, F.; Jayasekara, R.; Griffiths, I.; Gunatillake, P. Thermoplastic Biodegradable Polyurethanes, the Effect of Chain Extender Structure on Properties and *In Vitro* Degradation. *Biomaterials* **2007**, *28*, 5407−5417.
(45) Lee, C.; Grodzinsky, A.; Spector, M. The Effects of Cross-linking of Collagen-Glycosaminoglycan Scaffolds on Compressive Stiffness, Chondrocyte-Mediated Contraction, Proliferation and Biosynthesis. *Biomaterials* **2001**, *22*, 3145−3154.
(46) Berglund, J.; Mohseni, M.; Nerem, R.; Sambanis, A. A Biological Hybrid Model for Collagen-Based Tissue Engineered Vascular Constructs. *Biomaterials* **2003**, *24*, 1241−1254.
(47) Weadock, K.; Miller, E.; Bellincampi, L.; Zawadsky, J.; Dunn, M. Physical Crosslinking of Collagen Fibers: Comparison of Ultraviolet Irradiation and Dehydrothermal Treatment. *J. Biomed. Mater. Res.* **1995**, *29*, 1373−1379.
(48) Mallory; Sheehan; Hrapchak. *Histotechnology—A Self-Instructional Text*; American Society of Clinical Pathologists (ASCP) Press: Chicago, IL, 1990.
(49) Khait, L.; Birla, R. Bypassing the Patient: Comparison of Biocompatible Models for the Future of Vascular Tissue Engineering. *Cell Transplant.* **2012**, *21*, 269−283.
(50) Tondreau, M.; Laterreur, V.; Gauvin, R.; Vallières, K.; Bourget, J.; Lacroix, D.; Tremblay, C.; Germain, L.; Ruel, J.; Auger, F. Mechanical Properties of Endothelialized Fibroblast-derived Vascular Scaffolds Stimulated in a Bioreactor. *Acta Biomater.* **2015**, *18*, 176−185.
(51) Browning, M.; Dempsey, D.; Guiza, V.; Becerra, S.; Rivera, J.; Russell, B.; Höök, M.; Clubb, F.; Miller, M.; Fossum, T.; Dong, J.; Bergeron, A.; Hahn, M.; Cosgriff-Hernandez, E. Multilayer Vascular Grafts Based on Collagen-mimetic Proteins. *Acta Biomater.* **2012**, *8*, 1010−1021.
(52) Kumar, V.; Caves, J.; Haller, C.; Dai, E.; Liu, L.; Grainger, S.; Chaikof, E. Acellular Vascular Grafts Generated from Collagen and Elastin Analogs. *Acta Biomater.* **2013**, *9*, 8067−8074.
(53) Karimi, A.; Navidbakhsh, M.; Shojaei, A.; Faghihi, S. Measurement of the Uniaxial Mechanical Properties of Healthy and Atherosclerotic Human Coronary Arteries. *Mater. Sci. Eng., C* **2013**, *33*, 2550−2554.

DOI: 10.1021/acsami.5b03892
ACS Appl. Mater. Interfaces 2015, 7, 16202−16212